Nucleic Acids Research, 2024, **52**, D194–D202
https://doi.org/10.1093/nar/gkad691
Advance access publication date: 17 August 2023
Database issue

m^{6}A-Atlas v2.0: updated resources for unraveling the *N*^{6}-methyladenosine (m^{6}A) epitranscriptome among multiple species

Zhanmin Liang[1,2,†], Haokai Ye[2,3,†], Jiongming Ma[1,2,3,†], Zhen Wei[2,4,*], Yue Wang[5,6], Yuxin Zhang[1,2,3], Daiyun Huang[2,6], Bowen Song[7], Jia Meng[2,8,3], Daniel J. Rigden[3] and Kunqi Chen[1,*]

[1]Key Laboratory of Ministry of Education for Gastrointestinal Cancer, School of Basic Medical Sciences, Fujian Medical University, Fuzhou, Fujian 350004, China
[2]Department of Biological Sciences, Xi'an Jiaotong-Liverpool University, Suzhou, Jiangsu 215123, China
[3]Institute of Systems, Molecular and Integrative Biology, University of Liverpool, Liverpool L69 7ZB, Liverpool, UK
[4]Institute of Life Course and Medical Sciences, University of Liverpool, Liverpool L69 7ZB, UK
[5]Department of Mathematical Sciences, Xi'an Jiaotong-Liverpool University, Suzhou, Jiangsu 215123, China
[6]Department of Computer Science, University of Liverpool, Liverpool L69 7ZB, UK
[7]Department of Public Health, School of Medicine & Holistic Integrative Medicine, Nanjing University of Chinese Medicine, Nanjing 210023, China
[8]AI University Research Centre, Xi'an Jiaotong-Liverpool University, Suzhou, Jiangsu 215123, China

[*]To whom correspondence should be addressed. Tel: +86 0591 22862299; Email: kunqi.chen@fjmu.edu.cn
Correspondence may also be addressed to Zhen Wei. Email: zhen.wei01@xjtlu.edu.cn
[†]The authors wish it to be known that, in their opinion, the first three authors should be regarded as Joint First Authors.

Abstract

N^6-Methyladenosine (m^{6}A) is one of the most abundant internal chemical modifications on eukaryote mRNA and is involved in numerous essential molecular functions and biological processes. To facilitate the study of this important post-transcriptional modification, we present here m^{6}A-Atlas v2.0, an updated version of m^{6}A-Atlas. It was expanded to include a total of 797 091 reliable m^{6}A sites from 13 high-resolution technologies and two single-cell m^{6}A profiles. Additionally, three methods (exomePeaks2, MACS2 and TRESS) were used to identify >16 million m^{6}A enrichment peaks from 2712 MeRIP-seq experiments covering 651 conditions in 42 species. Quality control results of MeRIP-seq samples were also provided to help users to select reliable peaks. We also estimated the condition-specific quantitative m^{6}A profiles (i.e. differential methylation) under 172 experimental conditions for 19 species. Further, to provide insights into potential functional circuitry, the m^{6}A epitranscriptomics were annotated with various genomic features, interactions with RNA-binding proteins and microRNA, potentially linked splicing events and single nucleotide polymorphisms. The collected m^{6}A sites and their functional annotations can be freely queried and downloaded via a user-friendly graphical interface at: http://rnamd.org/m6a.

Received: July 17, 2023. **Revised:** August 2, 2023. **Editorial Decision:** August 4, 2023. **Accepted:** August 10, 2023

Graphical abstract

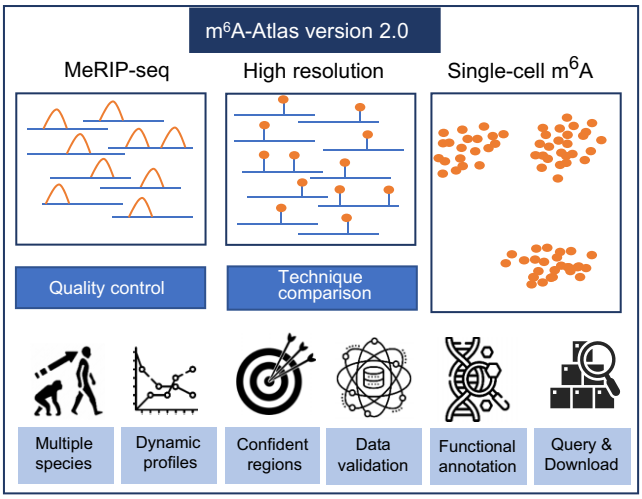

Introduction

N^6-Methyladenosine (m^6A) is the most abundant chemically modified nucleotide of mRNA in eukaryotes (1), which has also been observed on long non-coding RNA (lncRNA), tRNA and rRNA (2). The abundance of m^6A has been shown to be 0.1–0.4% of total adenosines in cellular RNA and tends to be present at the consensus DRACH (D = A\G\U; R = A\G; H = A\C\U) motifs (3). In addition, m^6A is typically enriched in 3′-untranslated regions (UTRs) and near the stop codons (4). The characteristic transcriptomic distribution patterns of m^6A methylation suggested its important roles in biological processes (4). Indeed, recent studies have revealed its roles in cell/embryo/neuron development (5–7), tumor development and metastasis (8–10), virus infection (11–13), virus-associated metastasis (14,15) and resistance to anti-tumor drugs (16,17).

In 2011, the fat mass and obesity-associated protein (FTO) was found to target and efficiently demethylate the m^6A residues in RNAs (18). Since then, the mechanism of dynamic m^6A regulation has been systematically studied (19). Methylation can be catalyzed by RNA methyltransferases in multicomponent complexes such as methyltransferase-like 3 (METTL3), methyltransferase-like 14 (METTL14) and Wilms tumor 1-associated protein (WTAP), and can be removed by demethylases, which have been discovered to include FTO and alkylated DNA repair protein AlkB homolog 5 (ALKBH5). Regulation also involves m^6A-binding proteins, such as YTH-domain family 1–3 (YTHDF1–3), YTHDC1 and YTHDC2, which exert regulatory functions through selective recognition. For instance, m^6A residues can influence the stability of target transcripts by interacting with YTHDF2 or promote protein synthesis by interacting with YTHDF1 (20).

In order to fully understand the function of m^6A, it is important to decipher the m^6A epitranscriptome profiles under specific cellular conditions. Multiple sequencing technologies were developed for this purpose, each with different features and strengths. MeRIP-seq/m^6A-seq is the most widely applied m^6A detection technique. It is an efficient method for condition-specific m^6A site identification, m^6A methylation level quantification and differential methylation comparison (4,21). Later, to compensate for the limited resolution (~100 bp) of MeRIP-seq, m^6A-CLIP/miCLIP was developed to profile m^6A sites under base resolution using the antibody cross-linking technique (22,23). The high-resolution detection technologies promoted further research on m^6A, such as the m^6A distribution in the nucleus and splicing (24), and its association with histone H3 trimethylation (25). Currently, at least 13 next-generation sequencing (NGS)-based technologies have been developed to provide epitranscriptome profiles with high resolution (26–29). In addition, the Oxford nanopore technique was also used to detect m^6A sites (30–32) which may provide isoform-specific m^6A profiles. Finally, in a recent study, scDART-seq was developed to enable the deconvolution of m^6A levels at the single-cell level (33).

To date, a number of bioinformatics databases for RNA modification have been constructed, including RMBase (34), REPIC (35) and MeT-DB (36), reporting modification sites, MODOMICS (37) which provides modification types, and other databases (38–42) which have summarized RNA modification-associated diseases or regulations. Among them, m^6A-Atlas (43), which was established in 2020, collected reliable m^6A sites obtained from seven high-resolution epitranscriptome profiling technologies, and integrated various post-transcriptional regulatory mechanisms to provide a more comprehensive view of the m^6A epitranscriptome. With the growing research focus on m^6A and the accumulation of NGS data, we improved m^6A-Atlas by including more sequencing techniques, peak calling methods and species. Also, to make it easier and more flexible for users to deal with results coming from different batches, we presented the quality control information for samples so that users can filter the results based on their knowledge.

- Enhanced coverage. (i) We collected 797 091 m^6A sites from seven species derived from 13 technologies with single base resolution. Additionally, another seven types of RNA modification reported by 16 kinds of techniques were summarized to show the potential interaction between different RNA modifications. (ii) Two single-cell m^6A profiles for human and mouse were obtained from scDART-seq and scm6A-seq, respectively. (iii) MeRIP-seq raw data were collected to identify m^6A-enriched regions from 42 species (including 12 viruses) and 651

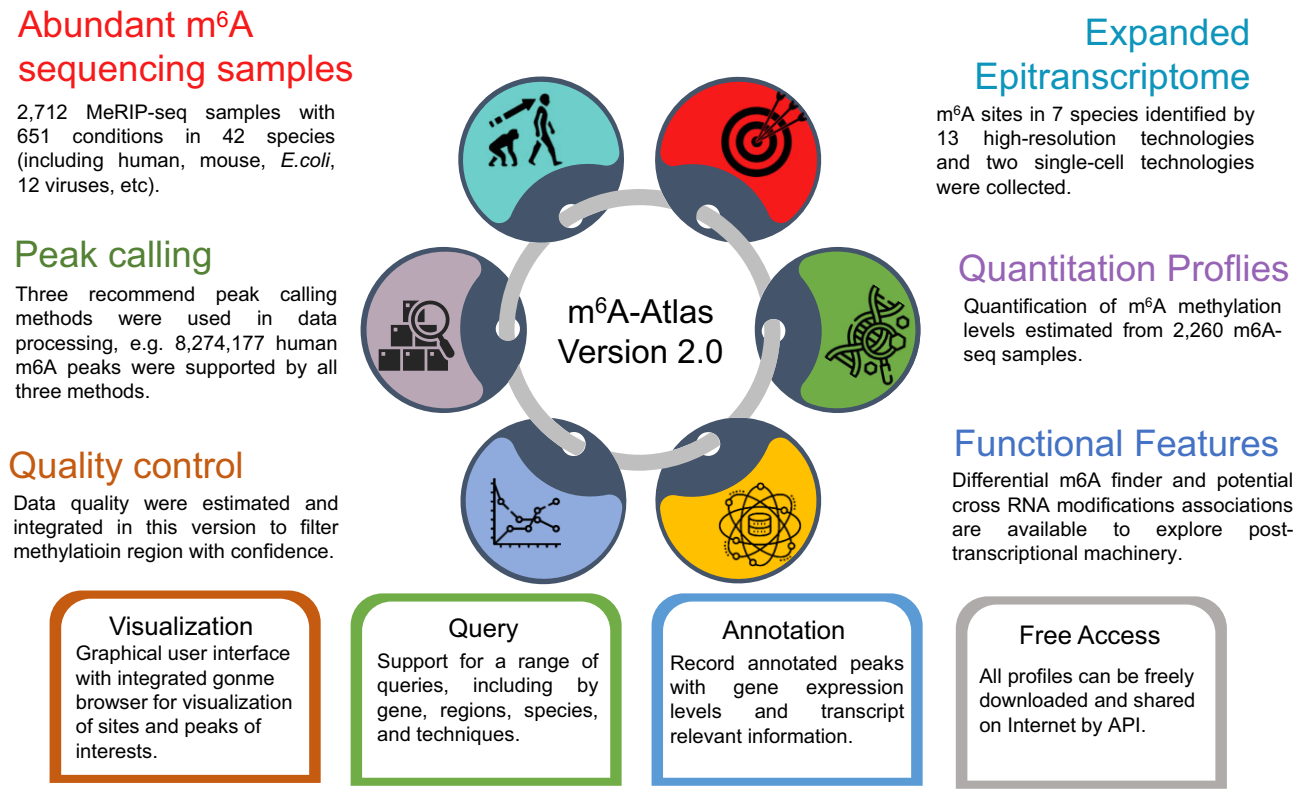

Figure 1. The overall design of m^{6}A-Atlas v2.0. m^{6}A-Atlas v2.0 is an updated version of m^{6}A-Atlas that provides m^{6}A profiles for 42 species with various resolutions. It also supports query of the quality of MeRIP-seq data, conservative sites, functional annotations of sites and identification of differentially methylated m^{6}A peaks under different conditions.

conditions. Three m^{6}A peak calling algorithms, namely exomePeak2 that was used in the first version of m^{6}A-Atalas, MACS2 and recent advanced TRESS (44–47), were used to call m^{6}A peaks from raw data. Results of the three methods were carefully integrated to provide 16 million m^{6}A enriched peaks.

- Quality control. In the updated version, 2712 MeRIP-seq samples produced from different laboratories and at different times were collected. Unwanted technical variation and differences across batches can hinder the integration of batches of data. To this end, we provided the quality control information for MeRIP-seq samples so that users could quickly select and filter the results by quality control metrics. Inspired by Zhang *et al.* (48), five metrics, namely GC content, mapping ratios, motif occurrence within peaks, number of 10-fold enriched peaks and relative distribution on transcripts were calculated. In terms of high-resolution m^{6}A profiles, sites could be filtered by techniques. A comprehensive comparison among different technologies were applied following pervious work (49); we found that sites with a false discovery rate (FDR) <0.05 were generally supported by more than four techniques. Therefore, for high-resolution m^{6}A profiles, sites reported by at least four techniques were considered as confident sites.

m^{6}A-Atlas v2.0 also provides a function that enables the query of differentially methylated m^{6}A peaks between different conditions from 19 species. A user-friendly graphical interface was constructed for the query of m^{6}A profiles and their functional features, involvement in the post-transcriptional machinery and conservation across vertebrates (i.e. human, mouse, rat and zebrafish). m^{6}A-Atlas v2.0 is freely accessible at http://rnamd.org/m6a and all searchable information can be downloaded from the webserver (see Figure 1).

Materials and methods

Collection of m^{6}A-enriched peaks

To identify m^{6}A-enriched peaks, 2712 MeRIP-seq samples, which cover 651 treatment conditions in 42 species, comprising 19 animals, 6 plants, 1 fungus (yeast), 2 apicomplexans, 2 prokaryotes and 12 viruses, were obtained from the NCBI GEO databases (50) and the GSA database (51) (see Supplementary Table S1 and S2). FastQC (v0.11.9) (52) was used to inspect the raw sequencing data and then adaptors and low-quality nucleotides were trimmed by TrimGalore (v0.6.6). Trimmed reads were mapped to the reference genome by HISAT2 (v2.2.1) (53) and the alignment results were converted to bam format file and sorted by SAMTools (v1.7) (54). Peak calling was performed on the mapped reads IP/input files using exomePeak2 (v1.2.0), MACS2 and TRESS (44–47). Condition-specific peaks called by the three methods were combined and peaks supported by multiple methods were highlighted. Additionally, differential m^{6}A methylation analysis is also available in the updated version.

Reference genome sequences were downloaded from Ensembl (55), NCBI (50), UCSC (56), the maizeDB database (57) and the GDR database (58). To ensure reliability, we performed a cross-validation between high-resolution m^{6}A sites and m^{6}A-enriched peaks. Meanwhile, the gene expression levels [transcripts per kilobase of exon model per million mapped

reads (TPM)] for the m^{6}A matched transcripts were also estimated from the aligned and sorted BAM files of MeRIP-seq input control samples; StringTie (59) with default parameters was used to calculate the TPM to facilitate comparative analysis.

MeRIP-seq data quality controls

Following the idea of Cistrome (48), five quality control metrics were calculated:

- GC content. FastQC(52) was used to evaluate whether the per sequence GC content of a sample is in line with normal distribution. For a specific condition, if more than half of its samples failed the GC content evaluation (i.e. do not follow normal distribution), it would be considered as failed.
- Mapping ratios. Mapping ratios are measured by the percentage of reads that map to the reference genome over total raw reads. A good mapping ratio should be >80%. HISAT2 (v2.2.1) (53) and SAMTools (v1.7) (54) were used to obtain the mapping ratios.
- Motif occurrence within peaks. m^{6}A modifications usually appear in consensus motifs [i.e. DRACH in eukaryotes/virus and GCCAG in prokaryotes (60)]. A high percentage of non-DRACH/GCCAG motifs within enriched peaks might suggest highly non-specific binding of m^{6}A antibodies.
- Number of 10-fold enriched peaks. The fold change of m^{6}A peaks >10 can be considered as confident peaks. In this study, the 10-fold enrichment peaks identified by two or more m^{6}A identification methods were counted. More 10-fold enriched peaks (> 500) indicate better quality of the MeRIP-seq sample.
- Relative distribution on transcripts. Previous studies have shown that m^{6}A peaks are usually enriched in coding sequences and UTRs of transcripts (21). If the majority of peak summits are located in coding regions and UTRs (>90%), the sample can be considered to have good quality.

Collection of high-resolution and single-cell RNA modification profiling

In m^{6}A-Atlas v2.0, high-resolution techniques refer to technologies with single-base resolution or single-cell resolution. A total of 109 conditions of 13 single-base resolution technologies (61–65) for seven species (i.e. human, mouse, rat, zebrafish, fly, Arabidopsis and yeast) and one sample of single-cell resolution technologies for human were incorporated in our database. The processed data were obtained from the NCBI GEO database (50) or from publications (see Supplementary Table S3).

Quantitative profiles for collected m^{6}A sites

In m^{6}A-Atlas v2.0, the quantification of the m^{6}A methylation level is provided for the high-resolution m^{6}A sites. We quantify the m^{6}A methylation levels through the calculation of IP over input fold enrichment using read counts on m^{6}A sites in different species. Firstly, in order to accurately quantify the m^{6}A methylation level from different biological conditions, only methylation sites confirmed by base-resolution data were considered. Next, we count the reads from BAM files of MeRIP-seq data over the selected m^{6}A sites. Only sites with reads count >5 are kept. For most MeRIP-seq libraries, fragmentation and immunoprecipitation were usually performed on the poly(A)-selected mRNA (4): therefore, it is recommended that users focus only on the m^{6}A sites on exonic regions.

Annotation of m^{6}A sites and peaks

In addition to the genomic coordinates of m^{6}A sites, m^{6}A-Atlas v2.0 also provides the methylation level, differential methylation profiles, splicing sites, microRNA (miRNA) target sites, RNA-binding protein (RBP)-binding sites and RNA subcellular localization to facilitate the investigation of the potential downstream regulatory mechanism of m^{6}A. In addition to relevant feature annotations, other modification types on the same exon of target m^{6}A site can be queried in the human and mouse sets. The splicing sites and RNA subcellular localization were obtained from the UCSC database (56) and RNALocate (66), respectively. The miRNA target sites and RBP-binding sites in human were retrieved from starBase (67) and POSTAR (68). The m^{6}A conservation among different species was annotated by ConsRM (69). Basic gene information (gene ID in Ensembl or Entrez Gene ID; gene name in SYMBLE format; gene region) for identified sites and peaks were obtained from Ensembl and NCBI gene annotation files (50,55), respectively.

Database and web interface implementation

The MySQL Database Management System was employed to store and manage all datasets in m^{6}A-Atlas v2.0. Hypertext Preprocessor (PHP) and JavaScript were used for developing the database query and user interface. The layout and rendering of the web interface were based on Hyper Text Markup Language (HTML) and Cascading Style Sheets (CSS). The query results can be visualized in various forms of statistical graphs using DataTables, ECharts and HighCharts. JBrowse was implemented to navigate all genomic tracks over the webserver (70). The cross-species comparison for RNA modifications was available in the database based on the JBrowse2.

Results

To explore the collected RNA modification sites and their annotations efficiently, a user-friendly web interface was developed for m^{6}A-Atlas v2.0. Multiple filtering options are also provided to help users to select m^{6}A modification sites under specific constraints. For example, users can choose peak calling results from MeRIP-seq data or high-resolution data.

More than 16 million m^{6}A-enriched regions detected from 2712 MeRIP-seq samples were collected in m^{6}A-Atlas v2.0 to provide a more comprehensive view of the known m^{6}A epitranscriptome in 42 species (Figure 2A), covering animals, plants, fungi, apicomplexans, prokaryotes and viruses. The m^{6}A regions supported by multiple peak calling methods were annotated, e.g. there are 8 274 177 human m^{6}A peaks supported by all three methods (Figure 2B). For each condition, the consistency of different peak calling results could be visualized in the website 'statistics' page (Figure 2C). The majority of the sample can pass the quality control (Figure 2D) and we also find a positive correlation between the percentage of consistent peaks and qualities (Figure 2E). All m^{6}A peaks were comprehensively annotated, including gene information, transcript location, methylation level (IP over input $\log_2$fold

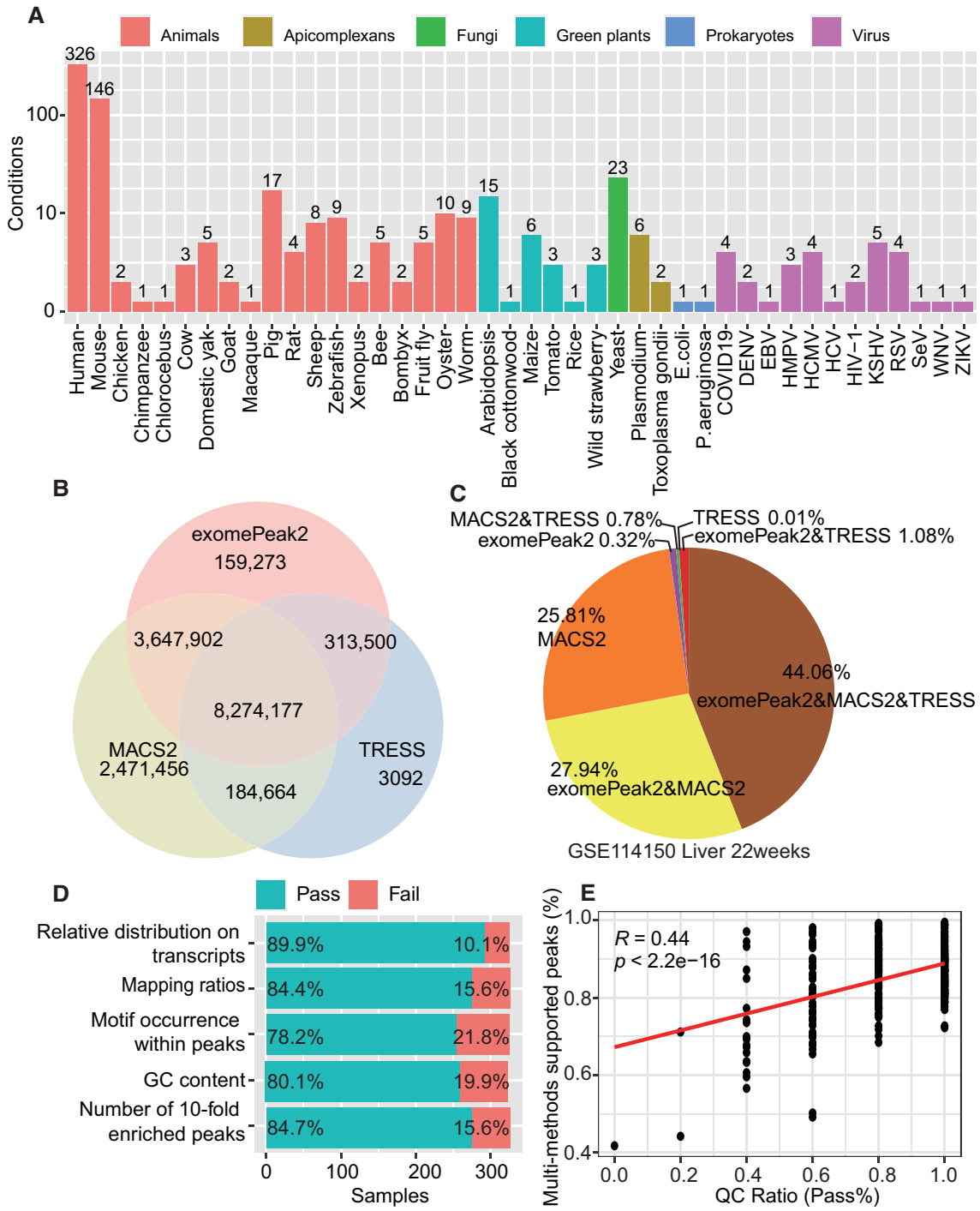

Figure 2. MeRIP-seq data and quality control in m^{6}A-Atlas v.2.0. (**A**) MeRIP-seq with 651 conditions stored in m^{6}A-Atlas v2.0. (**B**) More than 13 million human methylation peaks were identified and 60% of peaks were supported by three peak calling methods. (**C**) For each condition, the percentage of multi-method-supported peaks is available in the 'statistic' page, e.g. 73.86% of m^{6}A peaks were identified by at least two methods at condition 'GSE114150 Liver 22 weeks'. (**D**) The ratio of human samples passes the quality control. (**E**) The correlation between data quality and percentage of multi-method-supported m^{6}A peaks.

change), confidence score (–log *P*-value) and gene expression level.

Within the high-resolution repository, users can select their own species of interest and browse the m^{6}A modification sites and their interacting biological factors. In this update, by incorporating data from 13 single-base techniques covering seven species, we expanded the quantity of m^{6}A sites up to 797 091, including 427 760 human sites from 24 cell lines/tissues with 12 techniques. The consistency among different methods was estimated on all genes and housekeeping genes (Supplementary Table S4). Additionally, techniques could be divided two clusters, specifically the CLIP-based methods and antibody-free-based methods (Supplementary Figure S1). In addition, m^{6}A sites should be reported by at least four techniques to achieve an FDR <0.05 (Supplementary Table S5). Although some sites identified by certain techniques were difficult to reproduce, most of them could be verified by MeRIP-seq results (Supplementary Table S6).

Table 1. Key improvements of m^{6}A-Atlas v2.0 over existing databases

Techniques	Content	Met-DB v2.0	RMBase v2.0	REPIC	m^{6}A-Atlas V1.0	m^{6}A-Atlas V2.0
m^{6}A peaks from MeRIP-seq	Samples	138	>600	672	>1300	2712
	Eukaryotes	7	10	9	–	28
	Prokaryotes	–	2	2	–	2
	Virus	–	–	–	10	12
	Quality control	–	–	–	–	Yes
High-resolution data	Techniques	–	–	–	7	13
	Conditions	–	–	–	67	109
	Quantification	–	–	–	Yes	Yes
Single-cell m^{6}A profiles		–	–	–	–	Yes

Figure 3. Enhanced web interface of m^{6}A-Atlas v2.0. In this update, we provided quality control, tree diagram, genome browser, quantitative profiles, RBP and miRNA information and location of the other seven types of RNA modification to help in exploring the post-transcriptional machinery.

To help researchers explore relationships to other epitranscriptomics markers and the roles of m^{6}A in gene expression regulation and disease occurrence, genomic information including RBP, miRNA target, splicing site, single nucleotide polymorphism (SNP) annotation (40,71,72) and evolutionary conservation (69) were integrated in m^{6}A-Atlas v2.0. In general, m^{6}A-Atlas v2.0 provides the most comprehensive m^{6}A landscape among existing databases (Table 1).

Enhanced web interface and usage

For m^{6}A profiles from MeRIP-seq, the different quality control statistics for each condition are displayed. Users can quickly filter the results that passed (green) or failed (red) each quality control matrix. When we click a specific peak/site, a tree diagram that visualizes the supported conditions will appear, which may help us to identify condition-specific sites/peaks. In addition, we enhance the connectivity between MeRIP-seq data and high-resolution data; for each identified peak, overlapping m^{6}A peaks were annotated in the detail page. m^{6}A-Atlas v2.0 also offers graphic visualizations that display the position of the m^{6}A peaks/regions along the gene and genomic regions of interest, by genome browser. In the high-resolution sites page, the quantitative profile is available to show the dynamic methylation among different conditions. Also, the RBP and miRNA information were integrated in the websites to help in exploring the post-transcriptional machinery. Considering the potential interaction between different RNA modifications, the other seven types of modifications in the same exon are reported in the database for each m^{6}A site. All these features are summarized in Figure 3.

Tools: differential m^{6}A query and API

The differentially methylated region between selected pairs of treatment and control MeRIP-seq experiments can be found using differential m^{6}A-finder. In the tool module of the m^{6}A-Atlas v2.0 web server, users can compute the differential analysis result across cellular conditions after specifying the parameters of species, cell line and experiments. Furthermore, details of experimental data are also provided in the look-up table.

All source data in m^{6}A-Atlas v2.0, including low-resolution m^{6}A peaks and high-resolution m^{6}A sites and their functional annotations, can be freely accessed and shared. Users can also access the application program interface (API) on the web interface, which offers a personalized query and download of all collected data. Please refer to the 'API' pages for more complete data descriptions.

Discussion

With the recent advances in epitranscriptomics and high-throughput sequencing technologies, many high accuracy single-base resolution techniques have emerged for m^{6}A site detection. Meanwhile, the quantity of m^{6}A peak regions (e.g. MeRIP-seq) data has grown exponentially in recent years, providing an opportunity for the in-depth exploration of m^{6}A epitranscriptome data. Therefore, we have constructed an updated version of m^{6}A-Atlas to comprehensively integrate m^{6}A epitranscriptome profiles across different techniques and biological conditions. The m^{6}A enrichment regions that can be detected by multiple identification methods at the same time and can be queried by users as confident peaks, and statistics of five quality control metrics were provided to users for screening and filtering data. The database enables easy query, analysis and download of information. Moreover, by integrating annotation data from miRNA targets, splicing sites, RBP-binding sites, SNPs, evolutionary conservation and quantitative methylation levels, m^{6}A-Atlas v2.0 can be used to explore the relationships between RNA m^{6}A modification sites and other downstream functional features. In addition, the functionality of differential m^{6}A queries can report differential profiles of m^{6}A methylation between two biological conditions. In summary, m^{6}A-Atlas v2.0 provides a comprehensive and powerful knowledgebase for researchers to discover potential functional associations of m^{6}A epitranscriptomic modification and their mechanistic bases. In the future, we will continue to improve the depth and breadth of the data collection [such as m^{6}A sites detected by nanopore techniques (73)] and to maintain m^{6}A-Atlas v2.0 as a useful resource for the field.

Data availability

m^{6}A-Atlas v2.0 is an open-source collaborative initiative available on the Internet at http://rnamd.org/m6a/.

Supplementary data

Supplementary Data are available at NAR Online.

Acknowledgements

Author contributions: K.C. and Z.W. conceived the idea and initialized the project; Z.L. and Jiongming Ma collected and processed the epitranscriptome data in eukaryotes and viruses, respectively; H.Y. designed and built the m^{6}A-Atlas v2.0 website; Z.L. and H.Y. drafted the manuscript. All authors read, critically revised and approved the final manuscript.

Funding

The National Natural Science Foundation of China [32100519 and 31671373]; the XJTLU Key Program Special Fund [KSF-E-51 and KSF-*P*-02]; and the Scientific Research Foundation for Advanced Talents of Fujian Medical University [XRCZX202109].

Conflict of interest statement

None declared.

References

1. Jones,J.D., Monroe,J. and Koutmou,K.S. (2020) A molecular-level perspective on the frequency, distribution, and consequences of messenger RNA modifications. *Wiley Interdiscip. Rev. RNA*, **11**, e1586.
2. Meyer,K.D. and Jaffrey,S.R. (2017) Rethinking m^{6}A readers, writers, and erasers. *Annu. Rev. Cell Dev. Biol.*, **33**, 319–342.
3. Dubin,D.T. and Taylor,R.H. (1975) The methylation state of poly A-containing messenger RNA from cultured hamster cells. *Nucleic Acids Res.*, **2**, 1653–1668.
4. Dominissini,D., Moshitch-Moshkovitz,S., Schwartz,S., Salmon-Divon,M., Ungar,L., Osenberg,S., Cesarkas,K., Jacob-Hirsch,J., Amariglio,N., Kupiec,M., *et al.* (2012) Topology of the human and mouse m6A RNA methylomes revealed by m6A-seq. *Nature*, **485**, 201–206.

5. Kasowitz,S.D., Ma,J., Anderson,S.J., Leu,N.A., Xu,Y., Gregory,B.D., Schultz,R.M. and Wang,P.J. (2018) Nuclear m6A reader YTHDC1 regulates alternative polyadenylation and splicing during mouse oocyte development. *PLos Genet.*, **14**, e1007412.
6. Wang,D., Zhang,Z., Jiang,Y., Mao,Z., Wang,D., Lin,H. and Xu,D. (2021) DM3Loc: multi-label mRNA subcellular localization prediction and analysis based on multi-head self-attention mechanism. *Nucleic Acids Res.*, **49**, e46.
7. Cui,X., Liang,Z., Shen,L., Zhang,Q., Bao,S., Geng,Y., Zhang,B., Leo,V., Vardy,L.A., Lu,T., *et al.* (2017) 5-Methylcytosine RNA methylation in *Arabidopsis thaliana*. *Mol. Plant*, **10**, 1387–1399.
8. Shen,C., Sheng,Y., Zhu,A.C., Robinson,S., Jiang,X., Dong,L., Chen,H., Su,R., Yin,Z., Li,W., *et al.* (2020) RNA demethylase ALKBH5 selectively promotes tumorigenesis and cancer stem cell self-renewal in acute myeloid leukemia. *Cell Stem Cell*, **27**, 64–80.
9. Su,R., Dong,L., Li,Y., Gao,M., Han,L., Wunderlich,M., Deng,X., Li,H., Huang,Y., Gao,L., *et al.* (2020) Targeting FTO suppresses cancer stem cell maintenance and immune evasion. *Cancer Cell*, **38**, 79–96.
10. Zeng,L., Huang,X., Zhang,J., Lin,D. and Zheng,J. (2023) Roles and implications of mRNA N^6-methyladenosine in cancer. *Cancer Commun. (Lond.)*, **43**, 729–748.
11. Wang,B., Fang,X., Sun,X., Du,C., Zhou,L., Lv,X., Li,Y., Li,H. and Tang,W. (2021) m^6A demethylase ALKBH5 suppresses proliferation and migration of enteric neural crest cells by regulating TAGLN in Hirschsprung's disease. *Life Sci.*, **278**, 119577.
12. Liu,J., Xu,Y.P., Li,K., Ye,Q., Zhou,H.Y., Sun,H., Li,X., Yu,L., Deng,Y.Q., Li,R.T., *et al.* (2021) The m^6A methylome of SARS-CoV-2 in host cells. *Cell Res.*, **31**, 404–414.
13. Weng,H., Huang,H., Wu,H., Qin,X., Zhao,B.S., Dong,L., Shi,H., Skibbe,J., Shen,C., Hu,C., *et al.* (2018) METTL14 inhibits hematopoietic stem/progenitor differentiation and promotes leukemogenesis via mRNA m^6A modification. *Cell Stem Cell*, **22**, 191–205.
14. Ding,W.B., Wang,M.C., Yu,J., Huang,G., Sun,D.P., Liu,L., Zhang,J.N., Yang,Y., Liu,H., Zhou,W.P., *et al.* (2021) HBV/pregenomic RNA increases the stemness and promotes the development of HBV-related HCC through reciprocal regulation with insulin-like growth factor 2 mRNA-binding protein 3. *Hepatology*, **74**, 1480–1495.
15. Kim,G.W., Imam,H., Khan,M., Mir,S.A., Kim,S.J., Yoon,S.K., Hur,W. and Siddiqui,A. (2021) HBV-induced increased N6 methyladenosine modification of PTEN RNA affects innate immunity and contributes to HCC. *Hepatology*, **73**, 533–547.
16. Xu,J., Wan,Z., Tang,M., Lin,Z., Jiang,S., Ji,L., Gorshkov,K., Mao,Q., Xia,S., Cen,D., *et al.* (2020) N^6-Methyladenosine-modified CircRNA-SORE sustains sorafenib resistance in hepatocellular carcinoma by regulating β-catenin signaling. *Mol. Cancer*, **19**, 163.
17. Liu,X., Gonzalez,G., Dai,X., Miao,W., Yuan,J., Huang,M., Bade,D., Li,L., Sun,Y. and Wang,Y. (2020) Adenylate kinase 4 modulates the resistance of breast cancer cells to tamoxifen through an m^6A-based epitranscriptomic mechanism. *Mol. Ther.*, **28**, 2593–2604.
18. Jia,G., Fu,Y., Zhao,X., Dai,Q., Zheng,G., Yang,Y., Yi,C., Lindahl,T., Pan,T., Yang,Y.G., *et al.* (2011) N^6-Methyladenosine in nuclear RNA is a major substrate of the obesity-associated FTO. *Nat. Chem. Biol.*, **7**, 885–887.
19. Zhao,B.S., Roundtree,I.A. and He,C. (2017) Post-transcriptional gene regulation by mRNA modifications.. *Nat. Rev. Mol. Cell Biol.*, **18**, 31–42.
20. Wang,X., Zhao,B.S., Roundtree,I.A., Lu,Z., Han,D., Ma,H., Weng,X., Chen,K., Shi,H. and He,C. (2015) N^6-Methyladenosine modulates messenger RNA translation efficiency. *Cell*, **161**, 1388–1399.
21. Meyer,K.D., Saletore,Y., Zumbo,P., Elemento,O., Mason,C.E. and Jaffrey,S.R. (2012) Comprehensive analysis of mRNA methylation reveals enrichment in 3' UTRs and near stop codons. *Cell*, **149**, 1635–1646.
22. Ke,S., Pandya-Jones,A., Saito,Y., Fak,J.J., Vågbø,C.B., Geula,S., Hanna,J.H., Black,D.L., Darnell,J.E. Jr and Darnell,R.B. (2017) m^6A mRNA modifications are deposited in nascent pre-mRNA and are not required for splicing but do specify cytoplasmic turnover. *Genes Dev.*, **31**, 990–1006.
23. Linder,B., Grozhik,A.V., Olarerin-George,A.O., Meydan,C., Mason,C.E. and Jaffrey,S.R. (2015) Single-nucleotide-resolution mapping of m6A and m6Am throughout the transcriptome. *Nat. Methods*, **12**, 767–772.
24. Ke,S., Alemu,E.A., Mertens,C., Gantman,E.C., Fak,J.J., Mele,A., Haripal,B., Zucker-Scharff,I., Moore,M.J., Park,C.Y., *et al.* (2015) A majority of m6A residues are in the last exons, allowing the potential for 3' UTR regulation. *Genes Dev.*, **29**, 2037–2053.
25. Huang,H., Weng,H., Zhou,K., Wu,T., Zhao,B.S., Sun,M., Chen,Z., Deng,X., Xiao,G., Auer,F., *et al.* (2019) Histone H3 trimethylation at lysine 36 guides m^6A RNA modification co-transcriptionally. *Nature*, **567**, 414–419.
26. Hu,L., Liu,S., Peng,Y., Ge,R., Su,R., Senevirathne,C., Harada,B.T., Dai,Q., Wei,J., Zhang,L., *et al.* (2022) m^6A RNA modifications are measured at single-base resolution across the mammalian transcriptome. *Nat. Biotechnol.*, **40**, 1210–1219.
27. Dierks,D., Garcia-Campos,M.A., Uzonyi,A., Safra,M., Edelheit,S., Rossi,A., Sideri,T., Varier,R.A., Brandis,A., Stelzer,Y., *et al.* (2021) Multiplexed profiling facilitates robust m6A quantification at site, gene and sample resolution. *Nat. Methods*, **18**, 1060–1067.
28. Meyer,K.D. (2019) DART-seq: an antibody-free method for global m^6A detection. *Nat. Methods*, **16**, 1275–1280.
29. Körtel,N., Rücklé,C., Zhou,Y., Busch,A., Hoch-Kraft,P., Sutandy,F.X.R., Haase,J., Pradhan,M., Musheev,M., Ostareck,D., *et al.* (2021) Deep and accurate detection of m6A RNA modifications using miCLIP2 and m6Aboost machine learning. *Nucleic Acids Res.*, **49**, e92.
30. Zhang,Y., Huang,D., Wei,Z. and Chen,K. (2022) Primary sequence-assisted prediction of m^6A RNA methylation sites from Oxford nanopore direct RNA sequencing data. *Methods*, **203**, 62–69.
31. Piechotta,M., Naarmann-de Vries,I.S., Wang,Q., Altmüller,J. and Dieterich,C. (2022) RNA modification mapping with JACUSA2. *Genome Biol.*, **23**, 115.
32. Leger,A., Amaral,P.P., Pandolfini,L., Capitanchik,C., Capraro,F., Miano,V., Migliori,V., Toolan-Kerr,P., Sideri,T., Enright,A.J., *et al.* (2021) RNA modifications detection by comparative Nanopore direct RNA sequencing. *Nat. Commun.*, **12**, 7198.
33. Tegowski,M., Flamand,M.N. and Meyer,K.D. (2022) scDART-seq reveals distinct m^6A signatures and mRNA methylation heterogeneity in single cells. *Mol. Cell*, **82**, 868–878.
34. Xuan,J.J., Sun,W.J., Lin,P.H., Zhou,K.R., Liu,S., Zheng,L.L., Qu,L.H. and Yang,J.H. (2018) RMBase v2.0: deciphering the map of RNA modifications from epitranscriptome sequencing data. *Nucleic Acids Res.*, **46**, D327–D334.
35. Liu,S., Zhu,A., He,C. and Chen,M. (2020) REPIC: a database for exploring the N^6-methyladenosine methylome. *Genome Biol.*, **21**, 100.
36. Liu,H., Wang,H., Wei,Z., Zhang,S., Hua,G., Zhang,S.W., Zhang,L., Gao,S.J., Meng,J., Chen,X., *et al.* (2018) MeT-DB V2.0: elucidating context-specific functions of N6-methyl-adenosine methyltranscriptome. *Nucleic Acids Res.*, **46**, D281–D287.
37. Boccaletto,P., Stefaniak,F., Ray,A., Cappannini,A., Mukherjee,S., Purta,E., Kurkowska,M., Shirvanizadeh,N., Destefanis,E. and Groza,P. (2022) MODOMICS: a database of RNA modification pathways. 2021 update. *Nucleic Acids Res.*, **50**, D231–D235.
38. Luo,X., Li,H., Liang,J., Zhao,Q., Xie,Y., Ren,J. and Zuo,Z. (2021) RMVar: an updated database of functional variants involved in RNA modifications. *Nucleic Acids Res.*, **49**, D1405–D1412.
39. Deng,S., Zhang,H., Zhu,K., Li,X., Ye,Y., Li,R., Liu,X., Lin,D., Zuo,Z. and Zheng,J. (2021) M6A2Target: a comprehensive database for targets of m6A writers, erasers and readers. *Brief. Bioinform.*, **22**, bbaa055.
40. Song,B., Tang,Y., Chen,K., Wei,Z., Rong,R., Lu,Z., Su,J., de Magalhães,J.P., Rigden,D.J. and Meng,J. (2020) m7GHub: deciphering the location, regulation and pathogenesis of internal

mRNA N7-methylguanosine (m7G) sites in human. *Bioinformatics*, **36**, 3528–3536.
41. Chen,K., Song,B., Tang,Y., Wei,Z., Xu,Q., Su,J., de Magalhães,J.P., Rigden,D.J. and Meng,J. (2021) RMDisease: a database of genetic variants that affect RNA modifications, with implications for epitranscriptome pathogenesis. *Nucleic Acids Res.*, **49**, D1396–D1404.
42. Song,B., Huang,D., Zhang,Y., Wei,Z., Su,J., Pedro de Magalhães,J., Rigden,D.J., Meng,J. and Chen,K. (2022) m6A-TSHub: unveiling the context-specific m^6A methylation and m^6A-affecting mutations in 23 human tissues. *Genomics Proteomics Bioinformatics*, https://doi.org/10.1016/j.gpb.2022.09.001.
43. Tang,Y., Chen,K., Song,B., Ma,J., Wu,X., Xu,Q., Wei,Z., Su,J., Liu,G. and Rong,R. (2021) m^6A-Atlas: a comprehensive knowledgebase for unraveling the N^6-methyladenosine (m^6A) epitranscriptome. *Nucleic Acids Res.*, **49**, D134–D143.
44. Meng,J., Cui,X., Rao,M.K., Chen,Y. and Huang,Y. (2013) Exome-based analysis for RNA epigenome sequencing data. *Bioinformatics*, **29**, 1565–1567.
45. Meng,J., Lu,Z., Liu,H., Zhang,L., Zhang,S., Chen,Y., Rao,M.K. and Huang,Y. (2014) A protocol for RNA methylation differential analysis with MeRIP-Seq data and exomePeak R/bioconductor package. *Methods*, **69**, 274–281.
46. Zhang,Y., Liu,T., Meyer,C.A., Eeckhoute,J., Johnson,D.S., Bernstein,B.E., Nusbaum,C., Myers,R.M., Brown,M., Li,W., *et al.* (2008) Model-based analysis of ChIP-seq (MACS). *Genome Biol.*, **9**, R137.
47. Guo,Z., Shafik,A.M., Jin,P. and Wu,H. (2022) Differential RNA methylation analysis for MeRIP-seq data under general experimental design. *Bioinformatics*, **38**, 4705–4712.
48. Zheng,R., Wan,C., Mei,S., Qin,Q., Wu,Q., Sun,H., Chen,C.-H., Brown,M., Zhang,X., Meyer,C.A., *et al.* (2019) Cistrome Data Browser: expanded datasets and new tools for gene regulatory analysis. *Nucleic Acids Res.*, **47**, D729–D735.
49. Huang,D., Chen,K., Song,B., Wei,Z., Su,J., Coenen,F., de Magalhães,J.P., Rigden,D.J. and Meng,J. (2022) Geographic encoding of transcripts enabled high-accuracy and isoform-aware deep learning of RNA methylation. *Nucleic Acids Res.*, **50**, 10290–10310.
50. Sayers,E.W., Beck,J., Bolton,E.E., Bourexis,D., Brister,J.R., Canese,K., Comeau,D.C., Funk,K., Kim,S., Klimke,W., *et al.* (2021) Database resources, of the National Center for Biotechnology Information. *Nucleic Acids Res.*, **49**, D10–D17.
51. Chen,T., Chen,X., Zhang,S., Zhu,J., Tang,B., Wang,A., Dong,L., Zhang,Z., Yu,C., Sun,Y., *et al.* (2021) The genome sequence archive family: toward explosive data growth and diverse data types. *Genomics Proteomics Bioinformatics*, **19**, 578–583.
52. Brown,J., Pirrung,M. and McCue,L.A.J.B. (2017) FQC dashboard: integrates FastQC results into a web-based, interactive, and extensible FASTQ quality control tool. *Bioinformatics*, **33**, 3137–3139.
53. Kim,D., Langmead,B. and Salzberg,S.L.J.N. (2015) HISAT: a fast spliced aligner with low memory requirements. *Nat. Methods*, **12**, 357–360.
54. Li,H., Handsaker,B., Wysoker,A., Fennell,T., Ruan,J., Homer,N., Marth,G., Abecasis,G. and Durbin,R.J.B. (2009) The sequence alignment/map format and samtools. *Bioinformatics*, **25**, 2078–2079.
55. Howe,K.L., Achuthan,P., Allen,J., Allen,J., Alvarez-Jarreta,J., Amode,M.R., Armean,I.M., Azov,A.G., Bennett,R., Bhai,J., *et al.* (2021) Ensembl 2021. *Nucleic Acids Res.*, **49**, D884–D891.
56. Navarro Gonzalez,J., Zweig,A.S., Speir,M.L., Schmelter,D., Rosenbloom,K.R., Raney,B.J., Powell,C.C., Nassar,L.R., Maulding,N.D., Lee,C.M., *et al.* (2021) The UCSC Genome Browser database: 2021 update. *Nucleic Acids Res.*, **49**, D1046–D1057.
57. Woodhouse,M.R., Cannon,E.K., Portwood,J.L., Harper,L.C., Gardiner,J.M., Schaeffer,M.L. and Andorf,C.M. (2021) A pan-genomic approach to genome databases using maize as a model system. *BMC Plant Biol.*, **21**, 385.
58. Jung,S., Lee,T., Cheng,C.-H., Buble,K., Zheng,P., Yu,J., Humann,J., Ficklin,S.P., Gasic,K., Scott,K., *et al.* (2019) 15 years of GDR: new data and functionality in the Genome Database for Rosaceae. *Nucleic Acids Res.*, **47**, D1137–D1145.
59. Pertea,M., Kim,D., Pertea,G.M., Leek,J.T. and Salzberg,S.L. (2016) Transcript-level expression analysis of RNA-seq experiments with HISAT, StringTie and Ballgown. *Nat. Protoc.*, **11**, 1650–1667.
60. Deng,X., Chen,K., Luo,G.Z., Weng,X., Ji,Q., Zhou,T. and He,C. (2015) Widespread occurrence of N6-methyladenosine in bacterial mRNA. *Nucleic Acids Res.*, **43**, 6557–6567.
61. Garcia-Campos,M.A., Edelheit,S., Toth,U., Safra,M., Shachar,R., Viukov,S., Winkler,R., Nir,R., Lasman,L., Brandis,A., *et al.* (2019) Deciphering the 'm^6A code' via antibody-independent quantitative profiling. *Cell*, **178**, 731–747.
62. Schwartz,S., Agarwala,S.D., Mumbach,M.R., Jovanovic,M., Mertins,P., Shishkin,A., Tabach,Y., Mikkelsen,T.S., Satija,R., Ruvkun,G., *et al.* (2013) High-resolution mapping reveals a conserved, widespread, dynamic mRNA methylation program in yeast meiosis. *Cell*, **155**, 1409–1421.
63. Chen,K., Luo,G.Z. and He,C. (2015) High-resolution mapping of N^6-methyladenosine in transcriptome and genome using a photo-crosslinking-assisted strategy. *Methods Enzymol.*, **560**, 161–185.
64. Zhang,Z., Chen,L.Q., Zhao,Y.L., Yang,C.G., Roundtree,I.A., Zhang,Z., Ren,J., Xie,W., He,C. and Luo,G.Z. (2019) Single-base mapping of m^6A by an antibody-independent method. *Sci. Adv.*, **5**, eaax0250.
65. Koh,C.W.Q., Goh,Y.T. and Goh,W.S.S. (2019) Atlas of quantitative single-base-resolution N^6-methyl-adenine methylomes. *Nat. Commun.*, **10**, 5636.
66. Cui,T., Dou,Y., Tan,P., Ni,Z., Liu,T., Wang,D., Huang,Y., Cai,K., Zhao,X., Xu,D., *et al.* (2022) RNALocate v2.0: an updated resource for RNA subcellular localization with increased coverage and annotation. *Nucleic Acids Res.*, **50**, D333–D339.
67. Li,J.H., Liu,S., Zhou,H., Qu,L.H. and Yang,J.H. (2014) starBase v2.0: decoding miRNA–ceRNA, miRNA–ncRNA and protein–RNA interaction networks from large-scale CLIP-Seq data. *Nucleic Acids Res.*, **42**, D92–D97.
68. Zhu,Y., Xu,G., Yang,Y.T., Xu,Z., Chen,X., Shi,B., Xie,D., Lu,Z.J. and Wang,P. (2019) POSTAR2: deciphering the post-transcriptional regulatory logics. *Nucleic Acids Res.*, **47**, D203–D211.
69. Song,B., Chen,K., Tang,Y., Wei,Z., Su,J., de Magalhães,J.P., Rigden,D.J. and Meng,J. (2021) ConsRM: collection and large-scale prediction of the evolutionarily conserved RNA methylation sites, with implications for the functional epitranscriptome. *Brief. Bioinform.*, **22**, bbab088.
70. Buels,R., Yao,E., Diesh,C.M., Hayes,R.D., Munoz-Torres,M., Helt,G., Goodstein,D.M., Elsik,C.G., Lewis,S.E., Stein,L., *et al.* (2016) JBrowse: a dynamic web platform for genome visualization and analysis. *Genome Biol.*, **17**, 66.
71. Liu,L., Song,B., Chen,K., Zhang,Y., de Magalhães,J.P., Rigden,D.J., Lei,X. and Wei,Z. (2021) WHISTLE server: a high-accuracy genomic coordinate-based machine learning platform for RNA modification prediction. *Methods*, **203**, 378–382.
72. Ma,J., Song,B., Wei,Z., Huang,D., Zhang,Y., Su,J., de Magalhães,J.P., Rigden,D.J., Meng,J. and Chen,K. (2022) m5C-Atlas: a comprehensive database for decoding and annotating the 5-methylcytosine (m5C) epitranscriptome. *Nucleic Acids Res.*, **50**, D196–D203.
73. Zhang,Y., Jiang,J., Ma,J., Wei,Z., Wang,Y., Song,B., Meng,J., Jia,G., de Magalhães,J.P., Rigden,D.J., *et al.* (2023) DirectRMDB: a database of post-transcriptional RNA modifications unveiled from direct RNA sequencing technology. *Nucleic Acids Res.*, **51**, D106–D116.

Received: July 17, 2023. **Revised:** August 2, 2023. **Editorial Decision:** August 4, 2023. **Accepted:** August 10, 2023